PHYSICAL REVIEW A VOLUME 60, NUMBER 1 JULY 1999

Neutral dissociation by non-Rydberg doubly excited states

P. Erman, A. Karawajczyk, E. Rachlew-Källne, J. Rius i Riu, M. Stankiewicz,* and K. Yoshiki Franzén
Physics Department I, Royal Institute of Technology, S-10044 Stockholm, Sweden

L. Veseth
Department of Physics, University of Oslo, N-0316 Oslo, Norway

(Received 22 January 1999)

Neutral photodissociation from N_2 has been studied in the range 20–30 eV by observing dispersed fluorescence from excited N fragments. From comparisons with calculations using many-body perturbation theory it follows that these fragmentations follow from predissociations of N_2 Rydberg series by a number of non-Rydberg doubly excited states. [S1050-2947(99)04007-X]

PACS number(s): 33.80.Gj, 31.50.+w, 33.70.Ca

I. INTRODUCTION

A great amount of experimental data concerning photodissociation and photoionization of N_2 have been collected using continuously tunable synchrotron light (cf. Ref. [1] and references given therein). Most of the structures in the photoionization spectra from the limit at an excitation energy $E_{\mathrm{exc}}=15.58\,\mathrm{eV}$ up to $E_{\mathrm{exc}}=18.75\,\mathrm{eV}$ are well understood in terms of autoionizations of the Rydberg series $R(X)$, $R(A)$, and $R(B)$ converging to the $N_2{}^+$ states *X*, *A*, and *B*, respectively. For $E_{\mathrm{exc}}\geqslant 19.4\,\mathrm{eV}$ the very weak $R(D)$ series occurs and for $E_{\mathrm{exc}}\geqslant 22.1\,\mathrm{eV}$ the weak $R(C)$ series is observable.

In addition to photoionization/photoabsorption measurements, fluorescence from N_2 following synchrotron light excitation has also been studied in numerous investigations (cf. Ref. [1] and references given therein). Apart from molecular $N_2{}^+$ emission bands, strong atomic NI UV emission (120 nm) was observed [1] at the threshold $E_{\mathrm{exc}}=20.09\,\mathrm{eV}$. As found in [1] this emission (NI $3s\ {}^4P\rightarrow 2p\ {}^4S^0$) as a function of E_{exc} shows the same discrete structure in the $E_{\mathrm{exc}}=20-30\,\mathrm{eV}$ region as the photoionization spectrum, i.e., originating from the Rydberg series $R(C)$ and $R(D)$.

Figure 1 shows low lying excited states of the neutral nitrogen atom formed by excitations $2p\rightarrow 3s({}^4P,{}^2P)$ and $2p\rightarrow 3p({}^4S^0,{}^4P^0,{}^4D^0,{}^2D^0)$ as well as the emission (λ nm) from these states. The zero point of the energy scale refers to the ground state of the N_2 molecule. Thus, the first structure observed [1] at $E_{\mathrm{exc}}=20.09\,\mathrm{eV}$ was attributed to predissociations of the N_2 Rydberg series $R(D)$, $n=3$ mediated by some unknown neutral state in N_2 having the limit $\mathrm{N(g.s.)}+\mathrm{N}(3s\,{}^4P)$. This excited $\mathrm{N}(3s\ {}^4P)$ state subsequently decays to N(g.s.) by strong $\lambda=120\,\mathrm{nm}$ resonance emission. At $E_{\mathrm{exc}}=20.44\,\mathrm{eV}$ predissociations might lead to the formation of $\mathrm{N}(3s\ {}^2P)$ and subsequent $\lambda=149\,\mathrm{nm}$ emission (Fig. 1) which was included in the undispersed fluorescence (115–200 nm) measurements [1]. At $E_{\mathrm{exc}}=20.68\,\mathrm{eV}$ $\mathrm{N}(2s2p^4\ {}^4P)$ (not shown in Fig. 1) could be formed, but the $\lambda=113.4\,\mathrm{nm}$ emission from this level was outside the sensitivity range of the detector. With increasing E_{exc} other structures were found and attributed to the Rydberg series $R(D)$ $n=4,5$ and $R(C)$ $n=4,5,\ldots$. A strong intensity increase of the UV emission was observed for $E_{\mathrm{exc}}\geqslant 21.5\,\mathrm{eV}$, i.e., at energies where excited nitrogen atoms in the $3p({}^4S^0,{}^4P^0,{}^4D^0,{}^2D^0,\ldots)$ states may be created via predissociations (Fig. 1). All the $3p$ quartet states decay to the $3s\ {}^4P$ state with subsequent $\lambda=120\,\mathrm{nm}$ resonance emission.

To investigate these predissociation processes it was decided to measure the dispersed fluorescence from N_2 in the $E_{\mathrm{exc}}\geqslant 21.5\,\mathrm{eV}$ range and look for possible NI multiplets. Neutral dissociation of N_2 has been extensively discussed in the literature in view of its important applications, for instance in the physics of the atmospheres of the planets and the sun as well as in plasma physics. As an example molecu-

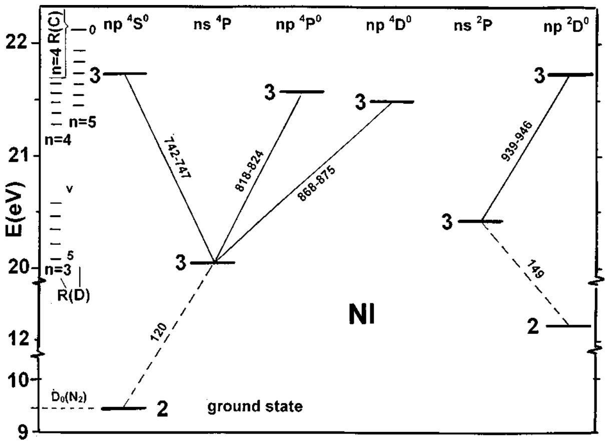

FIG. 1. Atomic transitions (λ nm) in neutral nitrogen observed at direct photon excitation in the range 20–28 eV from the ground state in the N_2 molecule (=zero point in the energy scale). The dashed transitions have been observed in our earlier work [1] and the infrared multiplets (solid lines) are studied in the present work. From the measured excitation functions (Fig. 3) and from many body calculations (Fig. 4) we conclude that the observed excited N atoms follow from predissociations of the N_2 Rydberg series $R(C)$ and $R(D)$ (displayed in the figure above) caused by non-Rydberg doubly excited states.

---

*Permanent address: Instytut Fizyki Mariana Smoluchowskiego, Jagiellonian University, Reymonta 4, Kraków, Poland.

©1999 The American Physical Society

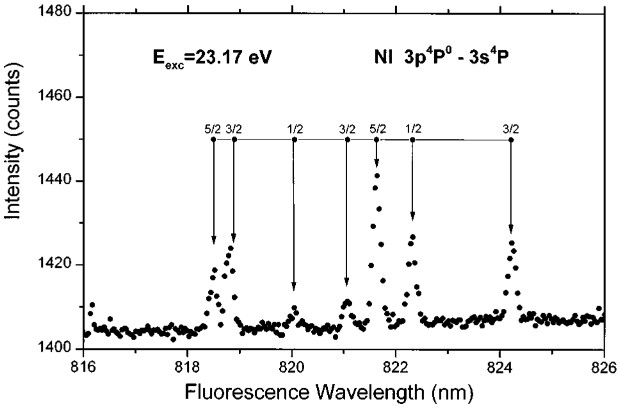

FIG. 2. The multiplet NI $3p\ ^4P^0 \rightarrow 3s\ ^4P$ recorded at a photon excitation energy $E_{\rm exc}=23.17$ eV. The well-resolved multiplet gives a unique fingerprint of the dissociation limit $\mathrm{N}(3p\ ^4P^0)$ $+\mathrm{N(g.s.)}$

lar collisions involving atomic nitrogen are known to have very high cross sections. However, studies of neutral photodissociation of N_2 have been concentrated to low photon excitation energies ($E_{\rm exc} \leqslant 15$ eV). For instance, it has been shown [2] that atomic nitrogen is formed in its lowest excited states $[2p^3(^2D^0,^2P^0)]$ following predissociations of higher lying (13.7–14.1 eV) valence states of N_2 by a postulated state $2\ ^3\Pi_u$.

II. EXPERIMENTS AND RESULTS

The experiments were performed by recording dispersed fluorescence emitted from N_2 molecules excited by monochromatized VUV photons from beam line 52 at the MAX synchrotron radiation facility in Lund, Sweden. The excitation energies utilized were in the 21–28.5 eV energy region with band widths ranging from 0.1 to 0.2 eV. The experimental setup included an interaction chamber with a glass window, a fluorescence light collecting system, a high throughput grating spectrometer with a CCD array detector. The photon beam entered via a differential pressure chamber into the interaction chamber with a background pressure lower than 5×10^{-6} Torr and a constant base pressure 3×10^{-2} Torr during measurements. The N_2 gas was of purity higher than 99.9%. The fluorescence light was collected by a lens system and directed into the spectrometer equipped with a 600 g/mm grating providing a wavelength dispersed image on the liquid nitrogen cooled CCD detector resulting in recorded low dark current spectra with a resolution in the range 0.2–1 nm in the interval 440–950 nm.

The four multiplets indicated in Fig. 1 were observed and the spectrum of the well resolved $3p\ ^4P^0 \rightarrow 3s\ ^4P$ multiplet is shown in Fig. 2. The excitation functions, i.e., the population of a given multiplet as a function of $E_{\rm exc}$ of the four multiplets, are shown in Fig. 3. as well as the energies of the primary excited $R(C)$ and $R(D)$ Rydberg series. It should be noted that there might be additional, but very small contributions from Rydberg series converging to the very recently discovered $2\ ^2\Pi_g$, $^2\Sigma_u$, $^2\Delta_u$ and $2\ ^2\Pi_u$ states in N_2^+ [3]. The excitation functions are arranged in the order of decreasing intensity. Thus $3p\ ^4P^0 \rightarrow 3s\ ^4P$ is by far the strongest multiplet and its excitation function (Fig. 3) shows a distinct

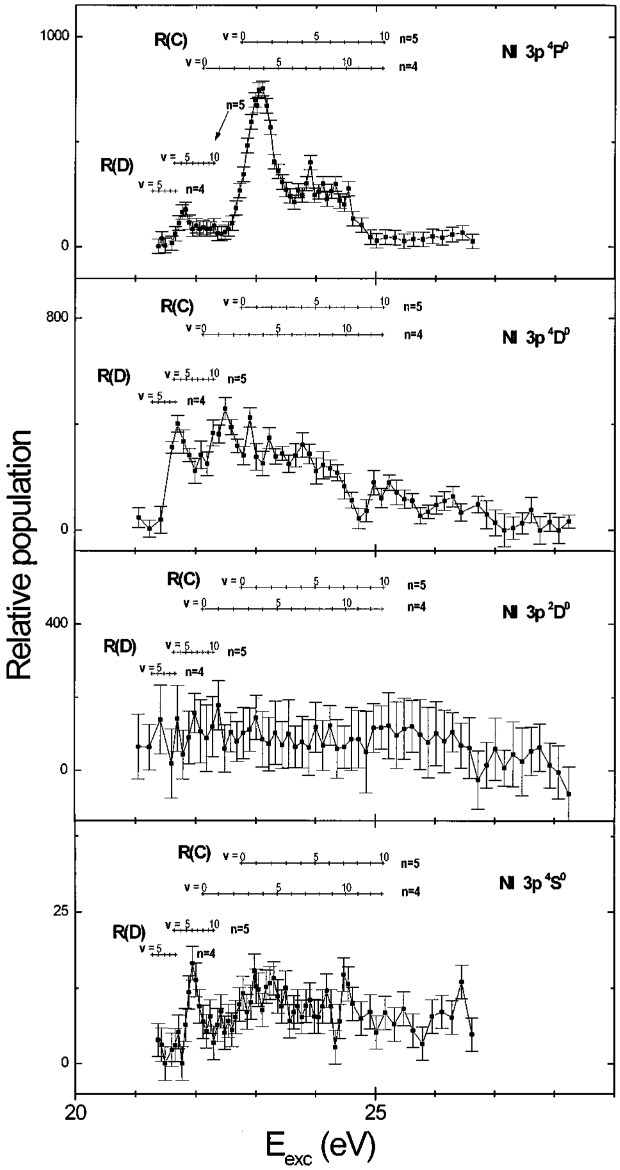

FIG. 3. Measured excitation functions of the $3p(^4P^0$, $^4D^0$, $^2D^0$, and $^4S^0)$ levels arranged in the order of decreasing populations. The positions of the precursing Rydberg levels of the $R(C)$ and $R(D)$ series in N_2 are indicated in the figures. The doublet splitting of the $R(D)$ levels are not shown.

vibrational structure around $E_{\rm exc}=24$ eV with a spacing roughly equal to that of the $R(C)$ series, which supports that the atomic emission follows from predissociations of the various vibrational levels of the Rydberg series $R(C)$ and $R(D)$.

III. THE NEUTRAL PHOTODISSOCIATION MECHANISM OF N_2 IN THE 20–30 eV REGION

To interpret the present experimental results we have made theoretical predictions to enable an identification of the states that cause the observed predissociations of the N_2 $R(C)$ and $R(D)$ series leading to the excited $3s(^2P,^4P)$ and $3p(^4S^0,^4P^0,^4D^0,^2D^0)$ levels in neutral nitrogen. The states of interest will dissociate into atomic products where one of the N atoms is expected to be in its ground state

$(1s^2 2s^2 2p^3\ {}^4S^0)$, whereas the other will be in an excited state characterized by a $2p \rightarrow 3p$ or a $2p \rightarrow 3s$ single excitation. Thus, we expect the relevant states to be of valence type, since molecular Rydberg states will converge to atomic fragments of higher energy.

Starting with the well-known Wigner-Witmer rules [4,5] for correlating atomic and molecular states in the diatomic case, we have worked out the number of molecular states of a specific symmetry that correlate with a given dissociation product. The number of molecular states of a given symmetry to be considered is then obtained simply by counting from the ground state dissociation products and upwards. The correlation with molecular states is finally performed in the standard way by observing the noncrossing rule, and the adiabatic principle which ensures that the symmetry labels are conserved at all internuclear separations. The molecular states that undergo predissociation are reached by electric dipole transitions from the $N_2 X\ {}^1\Sigma_g^+$ ground state. This means that the states of interest will be of ${}^1\Sigma_u^+$ or ${}^1\Pi_u$ symmetry. Thus, according to well-known selection rules, the states causing the predissociations have to be of ${}^1\Sigma_u^+$, ${}^1\Sigma_u^-$, ${}^1\Pi_u$ or ${}^1\Delta_u$ symmetry. However, spin conservation is not strict in predissociation, so triplet states have to be considered as well.

Vertical energies for the relevant singlet and triplet states at the ground state equilibrium internuclear separation ($R_e = 2.068$ a.u.) have been computed by a general multireference many-body method [6]. The computed results are visualized in Fig. 4. There are for instance just two states of relevant symmetry that converge to the N(g.s.)+N($3p\ {}^4S^0$) dissociation products at 21.75 eV, i.e., one ${}^1\Sigma_u^+$ and one ${}^3\Sigma_u^+$ state with vertical excitation energies 17.7 and 23.9 eV, respectively. Hence, the ${}^1\Sigma_u^+$ state is energetically not relevant, whereas the ${}^3\Sigma_u^+$ state seems promising and may yield a weak predissociation, in fact the only candidate that leads to this specific dissociation limit. From Fig. 4 we see that there are two singlet states leading to the N(g.s.)+N($3p\ {}^4P^0$) dissociation limit, i.e., one of ${}^1\Sigma_u^-$ symmetry at 24.0 eV, and one of ${}^1\Pi_u$ symmetry at 23.7 eV. Both are thus energetically promising candidates that may lead to strong spin-allowed predissociations. We have not included triplet states that lead to this dissociation limit.

All states that may cause predissociations considered in the present investigation are non Rydberg doubly excited resonances (NRDER's), with one excitation to the $1\pi_g$ lowest excited molecular orbital, and the other to a higher orbital of valence type. In a recent experimental work using synchrotron light excitation [7] such NRDER's were revealed in the 19–34 eV region in N_2. These states autoionize on the fs regime into the ${N_2}^+$ B state and were observed by measuring the vibrational branching ratio ($v' = 1/v' = 0$) of the subsequent ${N_2}^+$ $(B-X)$ emission. Follow-up many-body perturbation calculations [6] showed the symmetries and configurations of the observed NRDER's in N_2. Similar dispersed fluorescence measurements of branching ratios in CO also showed the existence of NRDER's in CO [8]. Very recent $(e,2e)$ experiments [9] have confirmed the existence of NRDER's in N_2 at the same energies as found in the fluorescence measurements [7].

The NRDER's observed so far [7–9] have symmetries which allow a photon excitation from the molecular ground states. The NRDER's observed in the present work have other symmetries and are observed in a two step process where they act as mediators of predissociations of primary excited Rydberg states.

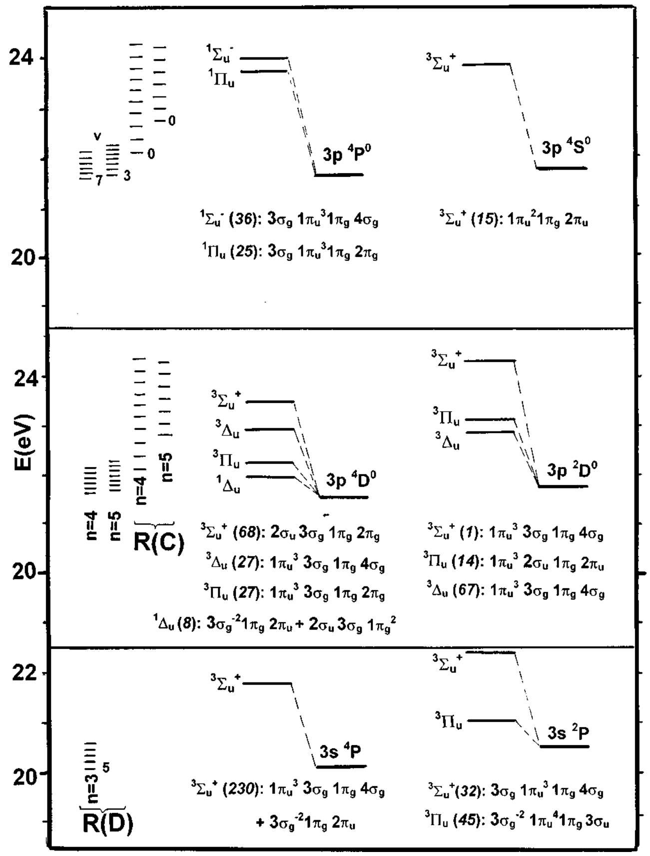

FIG. 4. Calculated vertical energies of non-Rydberg doubly excited resonances (NRDER's) in N_2 of various configurations causing predissociations of the N_2 Rydberg series $R(C)$ and $R(D)$ leading to the observed populations of the $3p({}^4S^0, {}^4P_0, {}^4D^0, {}^2D^0)$ and $3s({}^4P, {}^2P)$ levels in the neutral nitrogen atom. The numbers within the brackets are the calculated autoionization lifetimes (in fs) of the various NRDER's.

All NRDER's shown in Fig. 4 are unstable against autoionization, and we have estimated their lifetimes at vertical excitation by use of a many-body method as outlined in [6]. The autoionization lifetimes (in fs) are given within brackets in Fig. 4. They are considerably longer than the calculated lifetimes [6] for NRDER's with allowed excitations from the N_2 ground state. A long lifetime is an indication that, after switching to a dissociating state, the molecular state will be stable enough to dissociate rather than undergo autoionization. The fact that the states may autoionize unfortunately means that accurate excitation energies are hard to compute, since the process of autoionization is characterized by a singularity in the perturbation expansion. In [6] the accuracy of the excitation energies was estimated to be about 0.5 eV. This problem very much hampers the calculation of reliable potential curves, and we have made computations only within the Franck-Condon region at vertical excitation. All states of present interest that are included in the figures have

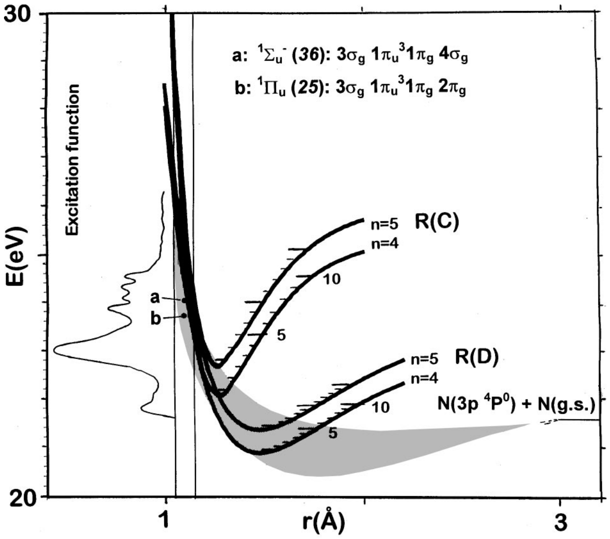

FIG. 5. Suggested shapes (hatched area) of the NRDER's ${}^1\Sigma_u^-(a)$ and ${}^1\Pi_u(b)$ with the dissociation limit N($3p\ {}^4P^0$) +N(g.s.). The shapes follow from the calculated points and slopes at the ground state equilibrium distance and the form of the inserted excitation functions, which demands the depicted crossing points with the Rydberg states $R(C)$ and $R(D)$.

rather large negative derivatives in this region, typically about -2.0 eV per 0.1 Å.

A more detailed information concerning the NRDER potential curves may be obtained by combining the results of the measured excitation functions, the calculated energies and slopes at $r=R_e$(g.s.) and the known dissociation limits. Figures 5 and 6 show the potential curves of the primary excited $R(C)$ and $R(D)$ ($n=4,5$) states including the $v=0-10$ vibrational levels. Figure 5 also includes the excitation function of the $3p\ {}^4P^0\rightarrow 3s\ {}^4P$ multiplet originating from the dissociation limit N($3p\ {}^4P^0$)+N(g.s.) at 21.60 eV of the postulated NRDER's with configurations a and b (see Fig. 5). The two calculated energies of a and b at $r=R_e$ are also included in Fig. 5 which suggest the shapes of the two NRDER's to be within the hatched area in Fig. 5, i.e., they should be attractive states with an equilibrium distance larger than that of $R(D)$. Thus the fact that the fluorescence starts at the 21.60 eV limit excludes repulsive states since such states would have to cross $R(D)$ far above the observed limit for the fluorescence. The predissociations of the Rydberg levels caused by a and b should take place in such a way that a maximum effect for the $R(D)$ levels occurs at around 21.7 eV and for the $R(C)$ at around 23 eV to explain the measured excitation function.

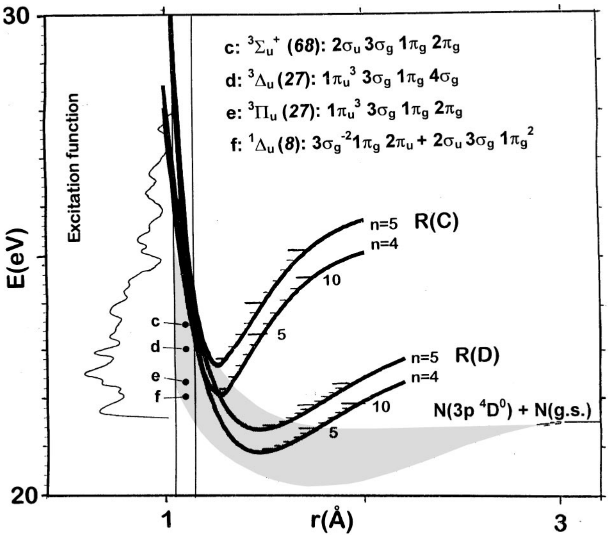

FIG. 6. Suggested shapes of the NRDER's ($c-f$) with the dissociation limit N($3p\ {}^4D^0$)+N(g.s.) based on the same discussion as in the Fig. 5 caption.

In Fig. 6 the excitation function of the $3p\ {}^4D^0\rightarrow 3s\ {}^4P$ multiplet is included as well as the calculated energies of the configurations $c-f$ (see Fig. 6) of the NRDER's having the limits N($3p\ {}^4D^0$)+N(g.s.). The shapes of the potential curves of these NRDER's are assumed to be within the hatched area in the figure, i.e., they should be attractive states with $R_e\geqslant 1.5$ Å for the same reasons as discussed above concerning Fig. 5. Since four NRDER's are involved in the formation of the N($3p\ {}^4D^0$) excitation function, the pattern of the latter is more complicated than that of the N($3p\ {}^4P^0$) excitation function. To understand the differences in the shapes of the N($3p\ {}^4P^0$) and N($3p\ {}^4D^0$) excitation functions, we have to consider the electron configurations of the Rydberg levels and the predissociating NRDER's.

The configurations of the $R(C)$ and $R(D)$ Rydberg levels are $3\sigma_g 1\pi_u^3 1\pi_g nl\lambda$ and $3\sigma_g^{-2}1\pi_u^4 1\pi_g nl\lambda$, respectively. The strongest observed predissociations lead to the N($3p\ {}^4P^0$) limit and are mediated by the spin-allowed interactions with the NRDER's ${}^1\Sigma_u^-$ and ${}^1\Pi_u$ whose configurations are $3\sigma_g 1\pi_u^3 1\pi_g 4\sigma_g$ and $3\sigma_g 1\pi_u^3 1\pi_g 2\pi_g$, respectively. These two configurations differ by just the one outermost electron from that of the $R(C)$ levels, which enables strong predissociation processes. However, these NRDER configurations differ from that of the $R(D)$ levels by two electrons and hence the predissociations to the N($3p\ {}^4P^0$) limit of the $R(D)$ levels should be considerably weaker than those of the $R(C)$ levels in agreement with the observations. The excitation function shows that predissociations to the N($3p\ {}^4D^0$) limit predominantly occurs at low excitation energies. The ${}^1\Delta_u$ state (f), which correlates with this limit, enables spin-allowed predissociations, and may be expected to account for this observation. It is also noted that the configuration of the ${}^1\Delta_u$ state when compared to that of the $R(C)$ and $R(D)$ levels favours an interaction with the latter levels in agreement with the experimental excitation function. For the other predissociations, that are all weak and caused by spin-forbidden interactions, the experimental evidence in favor of one or the other of the two Rydberg series is less clear. However, for the lowest limit $3s\ {}^4P$ predissociations are energetically possible only for the $R(D)$ series (Fig. 4). Since these predissociations are spin-forbidden, the subsequent $\lambda=120$ nm emission is weak until the threshold ($E_{\rm exc}\geqslant 21.5$ eV) is reached for spin-allowed predissociations leading to $3p({}^4P^0,{}^4D^0)$. The latter levels subsequently decay to $3s\ {}^4P$ (Fig. 1) yielding a strong increase of the $\lambda=120$ nm emission as observed in [1].

Direct dissociations to the limits under present study tend to be highly improbable. Electric dipole excitation from the N_2 ground state will lead to $^1\Sigma_u^+$ or $^1\Pi_u$ states, and the only singlet state that can be reached and which is able to dissociate to one of the actual limits is the doubly excited $^1\Pi_u$ state of Fig. 4. However, its electric dipole strength for transition from the ground state is computed to be as low as 0.028 a.u., which is about 50 times smaller than that of a typical single excitation. Finally it should be noted that no emission is observed from the higher lying NI multiplets $4p(^4S^0,^4P^0,^4D^0)$ (threshold $E_{\mathrm{exc}}=23.00\,\mathrm{eV}$). This suggests that, within the accuracy of the measurement, no predissociations of the $R(C)$ levels take place to these limits.

IV. SUMMARY

We have studied neutral photodissociation of N_2 from the threshold (20 eV) for the production of $2p\rightarrow 3s,3p$ excited nitrogen atoms up to about 30 eV. From the measured excitation functions and follow-up calculations we find that the neutral photodissociations follow from predissociations of the N_2 Rydberg series converging to the $C\ ^2\Sigma_u^+$ and $D\ ^2\Pi_{gi}$ states in $N_2{}^+$ by a set of attractive non-Rydberg doubly excited states. The strongest of the predissociation channels are mediated by doubly excited states of symmetry $^1\Pi_u$, $^1\Sigma_u^-$, and $^1\Delta_u$ leading to the limits $3p\ ^4P^0$ and $3p\ ^4D^0$, respectively.

[1] P. Erman, A. Karawajczyk, E. Rachlew-Källne, S. L. Sorensen, C. Strömholm, and M. Kirm, J. Phys. B **26**, 4483 (1993).

[2] C. W. Walter, P. C. Cosby, and H. Helm, J. Chem. Phys. **99**, 3553 (1993).

[3] H. Yoshii, T. Tanaka, Y. Morioka, T. Hayashi, and R. I. Hall, J. Mol. Spectrosc. **186**, 155 (1997).

[4] E. Wigner and E. Witmer, Z. Phys. **51**, 859 (1928).

[5] L. D. Landau and E. M. Lifshitz, *Quantum Mechanics*, 3rd ed. (Pergamon, Oxford, 1962).

[6] P. Sannes and L. Veseth, Phys. Rev. A **56**, 2893 (1997).

[7] P. Erman, A. Karawajczyk, U. Köble, E. Rachlew, K. Yoshiki Franzen, and L. Veseth, Phys. Rev. Lett. **76**, 4136 (1996).

[8] P. Erman, A. Karawajczyk, E. Rachlew-Källne, M. Stankiewicz, K. Yoshiki Franzen, P. Sannes, and L. Veseth, Phys. Rev. A **55**, 4221 (1997).

[9] R. Flammini, E. Fainelli, and L. Avaldi, (unpublished).